Human Reproduction, Vol.32, No.9 pp. 1892–1902, 2017
Advanced Access publication on July 20, 2017 doi:10.1093/humrep/dex244

human reproduction

ORIGINAL ARTICLE ***Reproductive endocrinology***

Combined androgen excess and Western-style diet accelerates adipose tissue dysfunction in young adult, female nonhuman primates

Oleg Varlamov[1,*], Cecily V. Bishop[2], Mithila Handu[1], Diana Takahashi[1], Sathya Srinivasan[1], Ashley White[1], and Charles T. Roberts Jr.[1,2,3]

[1]Division of Cardiometabolic Health, Oregon National Primate Research Center, 505 NW 185th Avenue, Beaverton, OR 97006, USA [2]Division of Reproductive & Developmental Sciences, Oregon National Primate Research Center, 505 NW 185th Avenue, Beaverton, OR 97006, USA [3]Department of Medicine, Oregon Health & Science University, 3181 SW Sam Jackson Park Road, Portland, OR 97239, USA

*Correspondence address. Oregon National Primate Research Center, 505 NW 185th Avenue, Beaverton, OR 97006, USA. Email: varlamov@ohsu.edu

Submitted on April 17, 2017; resubmitted on June 16, 2017; accepted on June 26, 2017

STUDY QUESTION: What are the separate and combined effects of mild hyperandrogenemia and consumption of a high-fat Western-style diet (WSD) on white adipose tissue (WAT) morphology and function in young adult female nonhuman primates?

SUMMARY ANSWER: Combined exposure to mild hyperandrogenemia and WSD induces visceral omental (OM-WAT) but not subcutaneous (SC-WAT) adipocyte hypertrophy that is associated with increased uptake and reduced mobilization of free fatty acids.

WHAT IS KNOWN ALREADY: Mild hyperandrogenemia in females, principally in the context of polycystic ovary syndrome, is often associated with adipocyte hypertrophy, but the mechanisms of associated WAT dysfunction and depot specificity remain poorly understood.

STUDY DESIGN, SIZE AND DURATION: Female rhesus macaques were randomly assigned at 2.5 years of age (near menarche) to receive either cholesterol (C; $n = 20$) or testosterone (T; $n = 20$)-containing silastic implants to elevate T levels 5-fold above baseline. Half of each of these groups was then fed either a low-fat monkey chow diet or WSD, resulting in four treatment groups (C, control diet; T alone; WSD alone; T + WSD; $n = 10$/group) that were maintained until the current analyses were performed at 5.5 years of age (3 years of treatment, young adults).

PARTICIPANTS/MATERIALS, SETTING AND METHODS: OM and SC-WAT biopsies were collected and analyzed longitudinally for *in vivo* changes in adipocyte area and blood vessel density, and *ex vivo* basal and insulin-stimulated fatty acid uptake and basal and isoproterenol-stimulated lipolysis.

MAIN RESULTS AND THE ROLE OF CHANCE: In years 2 and 3 of treatment, the T + WSD group exhibited a significantly greater increase in OM adipocyte size compared to all other groups ($P < 0.05$), while the size of SC adipocytes measured at the end of the study was not significantly different between groups. In year 3, both WAT depots from the WSD and T + WSD groups displayed a significant reduction in local capillary length and vessel junction density ($P < 0.05$). In year 3, insulin-stimulated fatty acid uptake in OM-WAT was increased in the T + WSD group compared to year 2 ($P < 0.05$). In year 3, basal lipolysis was blunted in the T and T + WSD groups in both WAT depots ($P < 0.01$), while isoproterenol-stimulated lipolysis was significantly blunted in the T and T + WSD groups only in SC-WAT ($P < 0.01$).

LIMITATIONS, REASONS FOR CAUTION: At this stage of the study, subjects were still relatively young adults, so that the effects of mild hyperandrogenemia and WSD may become more apparent with increasing age.

WIDER IMPLICATIONS OF THE FINDINGS: The combination of mild hyperandrogenemia and WSD accelerates the development of WAT dysfunction through T-specific (suppression of lipolytic response by T), WSD-dependent (reduced capillary density) and combined

T + WSD (increased fatty acid uptake) mechanisms. These data support the idea that combined hyperandrogenemia and WSD increases the risk of developing obesity in females.

STUDY FUNDING/COMPETING INTEREST(S): Research reported in this publication was supported by the Eunice Kennedy Shriver National Institute of Child Health and Human Development of the National Institutes of Health under award number P50 HD071836 to C.T. R. and award number OD 011092 from the Office of the Director, National Institutes of Health, for operation of the Oregon National Primate Research Center. The content is solely the responsibility of the authors and does not necessarily represent the official views of the National Institutes of Health.

Key words: PCOS / Western-style diet / nonhuman primates / hyperandrogenemia / obesity / androgen / testosterone / adipose tissue / lipolysis / fatty acid

Introduction

Polycystic ovary syndrome (PCOS) is a common disorder of reproductive age associated with ovarian dysfunction and infertility, which results in metabolic disturbances (Solomon, 1999) such as obesity and insulin resistance (IR) (Wagenknecht *et al.*, 2003; Escobar-Morreale and San Millan, 2007; Diamanti-Kandarakis and Dunaif, 2012). The diagnosis of PCOS has evolved over time, with the original NIH criteria requiring clinical or biochemical hyperandrogenism and evidence of oligo-ovulation and the exclusion of other disorders. The subsequent Rotterdam criteria required two out of three symptoms (hyperandrogenemia, oligo- or anovulation or polycystic ovaries), while the later Androgen Excess/PCOS Society criteria specified excess androgen levels, altered ovulation and/or polycystic ovaries and exclusion of other disorders (Rosenfield and Ehrmann, 2016).

Hyperandrogenemia is the most common primary diagnostic parameter in all cases, however. Mild (3 to 4-fold elevation) hyperandrogenemia can present as early as adolescence and persists into adulthood (Burt Solorzano *et al.*, 2012). While hyperandrogenemia is reported to play a central role in the pathogenesis of IR in PCOS women (Azziz *et al.*, 2009; Diamond *et al.*, 1998; Polderman *et al.*, 1994), its mechanisms with regard to female metabolism remain poorly understood. Weight loss can reduce ovarian and metabolic dysfunction (Barber and Franks, 2013; Lim *et al.*, 2013), resulting in improved insulin sensitivity and reduced hyperandrogenemia (Pasquali *et al.*, 1989; Holte *et al.*, 1995; Gambineri *et al.*, 2004; Mehrabani *et al.*, 2012; Thomson *et al.*, 2008), suggesting that obesity may exaggerates hyperandrogenemia-related symptoms in PCOS patients.

Clinical and animal studies demonstrated that PCOS and hyperandrogenemia are associated with the development of white adipose tissue (WAT) dysfunction characterized by local IR (Ciaraldi *et al.*, 1992; Ciaraldi *et al.*, 2009; Dunaif *et al.*, 1992), low-grade inflammation (Spritzer *et al.*, 2015), reduced insulin-mediated inhibition of lipolysis (Marsden *et al.*, 1994; Moro *et al.*, 2009), increased intra-abdominal fat mass (Dumesic *et al.*, 2016) and abdominal subcutaneous (SC) adipocyte hypertrophy (Manneras-Holm *et al.*, 2011; Dumesic *et al.*, 2016). The WAT present in PCOS women exhibits increased expression of fatty acid transporters and reduced levels of hormone-sensitive lipase (HSL) (Seow *et al.*, 2009) and the insulin-dependent glucose transporter-4 (GLUT-4) (Chen *et al.*, 2013; Wu *et al.*, 2014). PCOS-related WAT dysfunction also includes altered adipokine secretion (Spritzer *et al.*, 2015), reduced expression of lipogenic and developmental genes (Chazenbalk *et al.*, 2012) and altered adipogenesis (Keller *et al.*, 2014). Although these studies demonstrated the development of multiple WAT alterations in the presence of hyperandrogenemia, it remains to be determined whether the observed changes are primarily the result of increased visceral adiposity, which is also associated with the PCOS phenotype (Manneras-Holm *et al.*, 2011; Dumesic *et al.*, 2016).

The development of nonhuman primate (NHP) models of PCOS (Abbott *et al.*, 2013) has provided valuable translational tools for delineating tissue-specific mechanisms contributing to PCOS-related pathologies in humans. Pilot studies employing chronic, mild elevation of androgen in prepubertal rhesus macaques maintained through young adulthood demonstrated that these female monkeys developed metabolic and ovarian dysfunction when exposed to a high-fat/calorie-dense Western-style diet (WSD) as young adults (Varlamov *et al.*, 2013; McGee *et al.*, 2014). These findings revealed, for the first time, that diet can directly modulate reproductive and metabolic symptoms associated with hyperandrogenemia. In the present study, prepubertal female rhesus macaques were maintained on a control diet or WSD in the presence or absence of chronically elevated testosterone (T) levels similar to those in young women predisposed to PCOS through puberty and into early reproductive age. We used this study design to address the hypothesis that androgen excess would accelerate WSD-induced WAT dysfunction and to delineate diet- and androgen-specific mechanisms of metabolic dysfunction.

Materials and Methods

Animals

This study was approved by the Oregon National Primate Research Center (ONPRC) Institutional Animal Care and Use Committee (IACUC) and conforms to current Office of Laboratory Animal Welfares (OLAW) regulations as stipulated in assurance number A3304-01. Female rhesus macaques were pair-housed, with the cage size adjusted to animal weight according to the USDA Cage Size Guide, eighth Edition, beginning at 2.5 years of age (n = 40). The experimental design is described in Fig. 1. Females were maintained on either a typical chow diet (n = 20) consisting of two daily meals of fiber-balanced monkey diet (15% calories from fat, 27% from protein and 59% from carbohydrates; no. 5052; Lab Diet, St. Louis, MO), supplemented with fruits and vegetables, or a WSD (n = 20), containing 36% calories from fat, 18% from protein and 45% from carbohydrates (TAD Primate Diet 5LOP, 5A1F, Lab Diet), as previously reported (Grayson *et al.*, 2010). Animals consumed chow or WSD *ad libitum*. Daily caloric intake was not statistically different between experimental groups at any time point examined in the study (True *et al.*, 2017); thus, the WSD is isocaloric. Subsets of females consuming each diet were randomly

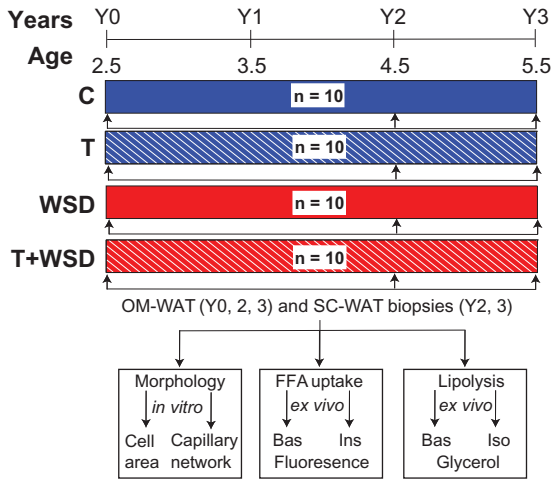

Figure 1 Study design. Female rhesus macaques were started at 2.5 years of age and maintained for 3 years on a standard chow or Western-style diet (WSD). The study involved four experimental groups: C, control animals; T, animals with chronically elevated testosterone (T) levels; WSD and T + WSD; n = 10/group (see the 'Results' section for details). Visceral omental-white adipose tissue (OM-WAT) biopsies were collected in years 0, 2 and 3, and subcutaneous (SC)-WAT biopsies in years 2 and 3. WAT biopsies were subjected to morphological analysis for the assessment of adipocyte size (cell area) and capillary network properties (see 'Materials and Methods' for details), and also analyzed *ex vivo* to quantify basal (Bas) and insulin-stimulated (Ins) fatty acid (FFA) uptake and lipolysis (glycerol release) under basal (Bas) and isoproterenol (Iso)-stimulated conditions.

selected to receive testosterone (T; n = 20) or cholesterol (C; n = 20) implants as reported elsewhere (McGee *et al.*, 2014). These treatments resulted in experimental groups designated chow + C (C), chow + T (T), C + WSD (WSD) and T + WSD (n = 10/ group). Androgen levels of T-treated animals were maintained 5-fold higher than control monkeys, which exceeds the 2-fold increase in T levels observed in post-pubertal women (Diamanti-Kandarakis and Panidis, 2007; Dumesic *et al.*, 2016). However, the T values achieved in the present study are similar to those observed in obese PCOS women (Eagleson *et al.*, 2003) (True *et al.*, 2017).

Wat biopsies

WAT biopsies were collected at the beginning of the study (year 0) and repeated annually (Fig. 1). In years 0 and 1, animals had small volumes of OM-WAT and had undeveloped SC-WAT, imposing some restrictions on a number of assays that could be conducted (see 'Results' for details). At the year 1 time point, animals exhibited no metabolic phenotype so WAT samples were not analyzed. WAT biopsies were collected by laparoscopy as previously described (Cameron *et al.*, 2016). In brief, anesthetized animals were positioned in dorsal recumbency followed by sterile preparation and draping of the abdomen. A Verres needle was inserted via a 1-cm subumbilical skin incision, followed by insufflation to 15 mm Hg pressure with CO_2 gas. The needle was removed and an 11-mm trocar/sheath and 10-mm telescope was inserted by puncture at the same site. A right paralumbar 5-mm accessory port was placed, through which a cutting biopsy grasper was inserted. Pinch-biopsy forceps were used to retrieve an OM-WAT biopsy from the falciform ligament. Grasping forceps were used to grab a small section of omentum, which was pulled through the side port and a 1 × 2 × 1 cm^3 tissue block was removed via sharp and blunt dissection. Abdominal SC-WAT biopsies were retrieved from the site of the scope incision. The abdomen was rinsed with warm saline, and the laparoscopic instruments were removed. The incision was closed with interrupted 4-0 Monocryl in the rectus fascia and skin.

Histological staining

At biopsy, 200–500-mg fragments of SC-WAT and OM-WAT were fixed in zinc formalin (Fisher Scientific, Hampton, NH, USA) at 4°C for 48 h, transferred to 70% (v/v) ethanol, embedded in Paraplast wax (Leica, Wetzlar, Germany) using a Tissue-Tek VIP six automatic tissue processor and embedding center (Sakura Finetek USA, Inc., Torrance, CA, USA), and 5-µm sections were prepared using on a micron rotary microtome. Slides were stained with a Masson Trichrome Stain Kit (IMEB Inc., San Marcos, CA, USA) according to the manufacturer's instructions. Images were acquired using an Olympus BX61VS slide scanner (Olympus, Tokyo, Japan) equipped with a ×20 UPLANSAPO NA 0.75 dry objective.

Lipolysis assay

At biopsy, 100 to 500-mg fragments of SC-WAT and OM-WAT were placed in 10 ml of M199 media (General Electric Company, Boston, MA, USA) at room temperature and transported to the laboratory within 30 min. 50 ± 5-mg WAT explants (three basal and three isoproterenol-stimulated replicates) were placed into a 48-well plate containing 0.2 ml incubation medium (Hank's Salt [HBSS], 0.2% BSA [Sigma-Aldrich, St, Louis, MO, USA] and 5 mM glucose), and incubated at 37°C free-floating for 2 h with or without 10 µM isoproterenol (Sigma-Aldrich) in an atmosphere with 5% CO_2 at 37°C. Glycerol release was determined using a glycerol detection kit (Sigma-Aldrich). Glycerol concentrations were calculated using glycerol standards (Sigma-Aldrich) and normalized to wet tissue weight.

Fluorescent fatty acid uptake and isolectin staining

At biopsy, 100–200 mg of WAT were collected in M199 media at room temperature and separated into smaller explants for two basal and two insulin-stimulated samples. WAT explants were incubated free-floating in a 48-well plate filled with 0.4 ml incubation medium (M199 medium, 0.1% (w/v) fatty acid-free BSA [Sigma-Aldrich], 20 mM HEPES [pH 7.4], supplemented with penicillin, streptomycin and fungizone, with or without 10 nM human insulin [Sigma-Aldrich]) for 2 h. Fluorescently labeled fatty acid BODIPY-500/510 C_1, C_{12} (BODIPY-C12; Life Technologies, Waltham, MA, USA) was prepared in advance by diluting a 2.5 mM methanol stock solution in incubation medium to a final concentration of 10 µM and incubated for 15 min, protected from light, in a 37°C water bath. One hundred µl of diluted BODIPY-C12 and 2 µl of live-cell staining dye Calcein Red-Orange AM (Life Technologies) were added to each well containing WAT explants and incubated for 15 min at 37°C. Media was removed by aspiration and explants were rapidly washed three times with incubation medium at 37°C and incubated in 0.4 ml basal or insulin-containing incubation medium for additional 30 min. This incubation step allows the translocation of BODIPY-C12 fluorescence associated with micro-lipid droplets (mLDs) into the interior of central lipid droplets (cLDs) and the incorporation of BODIPY-C12 into cellular triglycerides (Chu *et al.*, 2014; Varlamov *et al.*, 2015). Medium was removed by aspiration, the WAT explants were fixed at room temperature with 4% paraformaldehyde (Sigma-Aldrich) in PBS for 20 min, washed four times with PBS, and

stained, protected from light, for 1 h on a rocking platform with 20 µg/ml Isolectin GS-IB4, Alexa Fluor™ 647 conjugate (Life Technologies). Explants were washed four times with PBS and immediately analyzed by confocal microscopy. Each WAT explant triple-labeled with BODIPY-C12, calcein and isolectin was placed into a 35-mm glass-bottom imaging culture dish (MatTek, Ashland, MA) containing 100–200 µl of glycerol and sandwiched with the upper coverslip, allowing a tight contact between the outer layer of WAT explant and the bottom coverslip. Confocal microscopy was performed using a Leica SP5 AOBS spectral confocal system as described (Chu *et al.*, 2014) with the following modifications. Three-channel optical sections were collected in a sequential mode, at 2-µm intervals, using HC PL FLUOTAR 10.0 × 0.30 and ×20 PL APO NA 0.70 dry objectives.

Image analysis

Confocal optical sections were merged to generate the sum of z-projections using FIJI (https://imagej.net/Fiji/Downloads). Adipocyte area and single-cell BODIPY fluorescence (integrated density) were calculated semi-automatically using an open source Cell Magic Wand plugin for FIJI. Average adipocyte area in each animal was calculated as average values of 20–50 adipocytes per each depot. Blood vessel characteristics were assessed by isolectin channel using an open source software AngioTool as described (Zudaire *et al.*, 2011). Total vessel length in a WAT volume of 1550 µm × 1550 µm × 100 µm was calculated using ×10 images (sum of z-projections). Junction densities were calculated as a number of junctions in μm^2 of WAT.

Statistical analysis

OM-WAT adipocyte area and OM-WAT fatty acid uptake were analyzed using the Mixed Models function of SAS (version 9.4, SAS Institute Inc., Cary, NC, USA). Factors interrogated included time, steroid, diet, steroid by diet and steroid by diet by time. OM and SC-WAT glycerol release in years 2 and 3 of treatment was analyzed using the Linear Models function of SAS for each year individually. Factors interrogated included isoproterenol, diet, steroid and diet by steroid. SC-WAT adipocyte area, OM- and SC-WAT vessel and capillary junction density at year 3 were also analyzed using the Linear Models function of SAS. Factors interrogated included diet, steroid and diet by steroid. When significant ($P < 0.05$) factors were identified, all post-hoc analyses were then performed between relevant treatment groups using the least squared means function of SAS.

Results

Adipocyte size and wat morphology

The four treatment groups started with equally sized OM adipocytes that displayed progressive cellular hypertrophy over the course of the study (Fig. 2A). The C and T + WSD groups exhibited statistically significant increases in adipocyte size in years 2 and 3, while in the T group the increase in adipocyte size was only statistically significant when year 3 was compared to year 0. In the WSD group the increase in adipocyte size was statistically significant in year 2 but not in year 3. In years 2 and 3, the T + WSD group had statistically significantly larger OM adipocytes compared to all other groups (Fig. 2A). The morphological analysis of OM-WAT collected in year 2 showed no obvious signs of WAT fibrosis, with the exception of blood vessel-associated collagen beds (Fig. 2C). There was no significant difference in SC adipocyte size in year 3 (Fig. 2B). In year 3, in every experimental group, SC adipocytes were larger than OM adipocytes (Fig. 2A and B), which is consistent with previous human studies (Tchernof *et al.*, 2006; Michaud *et al.*, 2014; Muir *et al.*, 2016). Importantly, the relative difference in SC and OM adipocyte size was minimal in the T + WSD group compared to other groups (Fig. 2A and B).

Vessel density in WAT

Double-staining of BODIPY-C12-labeled (see next section) WAT explants collected in year 3 with Isolectin GS-IB4 revealed an extensive capillary network surrounding individual OM (Fig. 3A–D) and SC (data not shown) adipocytes. Typically, blood vessels formed junctions demarcating the boundaries between adjacent adipocytes (Fig. 3A–D, asterisks). Quantification of capillary length and junctions revealed that the overall effect of diet (WSD and T + WSD) on vessel length and junction densities was significant or a strong trend for both OM-WAT and SC-WAT and the WSD groups displayed reduced vessel length and junctional densities (Fig. 3E–H). Although OM adipocytes in the T + WSD group were larger compared to the WSD group (Figs 2A and 3 C and D), their capillary network properties, including vessel junction densities and vessel length, were similar (Fig. 3E and F). Similarly, WSD reduced vessel length and junction densities in SC-WAT (Fig. 3G and H).

Free fatty acid uptake in WAT

To analyze the uptake and incorporation of free fatty acids into cellular triglycerides, WAT explants were incubated *ex vivo* with basal or insulin-containing media and labeled with the green fluorescent fatty acid tracer BODIPY-C12, which is incorporated into cellular triglycerides (Chu, *et al.*, 2014; Varlamov *et al.*, 2015). Co-staining of BODIPY-C12-labeled OM-WAT explants with the live-cell marker Calcein Red-Orange AM revealed that only red, live adipocytes accumulated green fluorescent dye, while dead adipocytes (D) appeared dark (Fig. 4A and B). In live adipocytes, intracellular BODIPY fluorescence was distributed to clusters of small micro-lipid droplets (mLDs, Fig. 4A, punctate peripheral staining) and the central lipid droplet (cLD, Fig. 4A). An apparent intercellular heterogeneity in BODIPY-C12 uptake and mLDs (Figs 4A and 3A–D) were previously reported (Chu, *et al.*, 2014; Varlamov *et al.*, 2015). The quantification of basal and insulin-stimulated BODIPY-C12 fluorescence taken up by individual adipocytes showed no differences between treatment groups in year 2. However, only the T + WSD group demonstrated a statistically significant increase in the level of fatty acid uptake in year 3 compared to year 2 (Fig. 4C).

Lipolysis

The lipolytic response of WAT to the β-adrenergic agonist isoproterenol was studied *ex vivo* using WAT biopsies collected in years 2 and 3. In year 2, there were no statistically significant differences between treatment groups in isoproterenol-stimulated glycerol release in OM-WAT and SC-WAT (Fig. 5A and C, 'Iso'). In OM-WAT, there was a significant combined effect of diet and T on basal lipolysis, with the T + WSD group showing elevated basal glycerol release compared to the T group (Fig. 5A). In SC-WAT, due to a small number of biopsy samples collected, there were no group differences in basal lipolysis at year 2, although both WSD and T + WSD groups displayed a trend towards elevated basal lipolysis (Fig. 5C, 'Bas'). By year 3, the patterns of lipolytic responses changed dramatically compared to year 2. In both WAT depots and under both dietary conditions, there was a

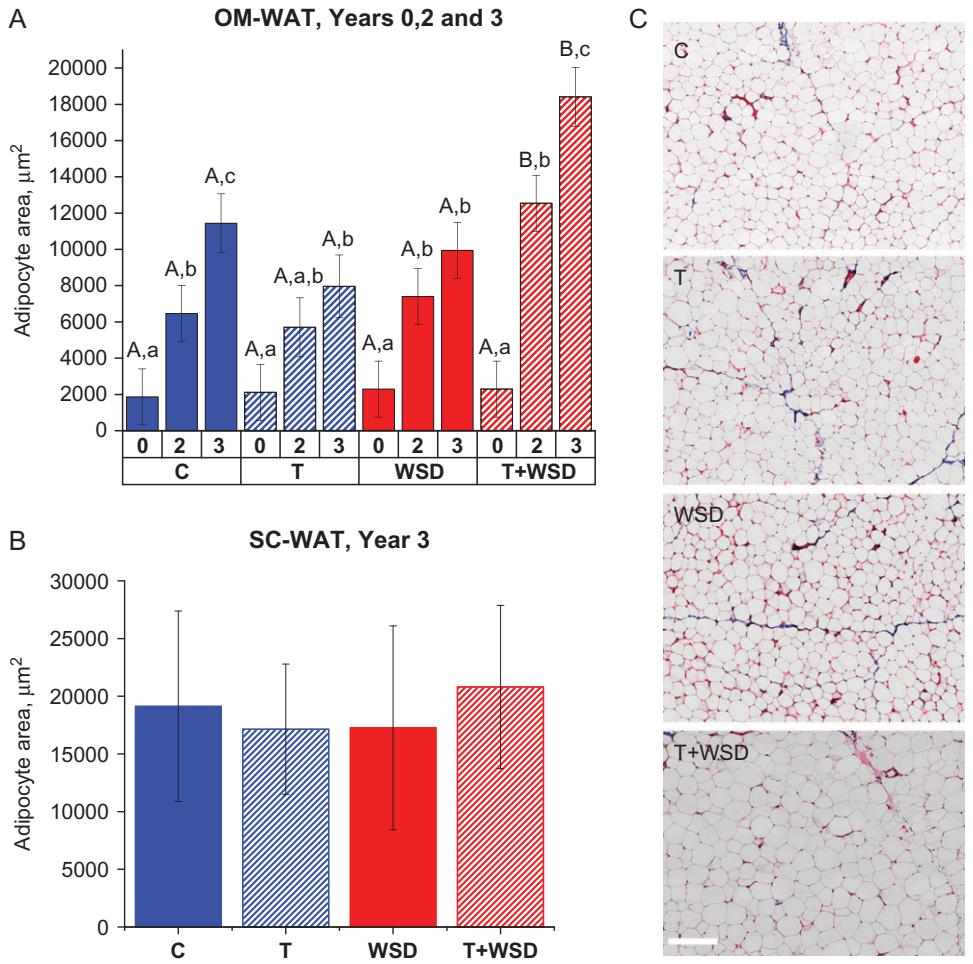

Figure 2 Adipocyte area and WAT morphology. Omental (OM) (**A**) and sub-cutaneous (SC) (**B**) adipocyte area was quantified in years 0, 2 and 3 for OM-white adipose tissue (WAT), and in year 3 for SC-WAT, as described in 'Materials and Methods.' Average cell area per animal was calculated for 20–50 adipocytes. (**C**) Representative examples of Trichrome-stained histological sections of OM-WAT (year 2). Pink color demarcates cellular membranes and cytoplasm, and blue color labels fibrotic structures (scale bar = 200 µm). (A) Uppercase letters denote differences ($P < 0.05$) by treatment within year, and lowercase letters indicate differences ($P < 0.05$) within a given treatment by year. (B) Analysis of SC-WAT area data was done for year 3 only with no difference detected by treatments ($P > 0.8$). Bars are means ± SEM.

significant inhibitory effect of T on basal glycerol release (Fig. 5B and D, 'Bas'). Also, both T and T + WSD groups displayed significantly reduced isoproterenol-stimulated glycerol release in SC-WAT and a trend towards reduction in OM-WAT (Fig. 5D and B, 'Iso').

Discussion

The present study was designed to discern the effects of WSD versus hyperandrogenemia on WAT function in young female NHPs, using a comprehensive approach of *ex vivo* and *in vitro* analyses of fat biopsies from two distinct fat depots. OM-WAT biopsies were collected longitudinally from the same anatomical sites, allowing the monitoring of the natural age-dependent progression of adipose hypertrophy, as well as the longitudinal assessment of various adipose-specific functions. The data from this study and a companion study (True *et al.*, 2017) suggest that the combination hyperandrogenemia and WSD accelerates the development of obesity (increase in BMI) and visceral WAT hypertrophy (increase in OM adipocyte area), while there were no significant effects of either treatment on SC-WAT hypertrophy (Fig. 2). Metabolic and WAT-specific changes became pronounced after 3 years of treatment, revealing several T-specific, diet-specific and combined effects of treatment, in that: (i) T inhibited basal and isoproterenol-stimulated lipolysis under both control diet and WSD conditions; (ii) WSD significantly reduced local WAT blood vessel length and junction densities, in the presence and absence of hyperandrogenemia; and (iii) only the combination of T and WSD resulted in increased insulin-dependent fatty acid uptake *ex vivo* (Table I).

Adipocyte size

The present study indicates that hyperandrogenemia in the context of an obesogenic diet is associated with the development of enlarged

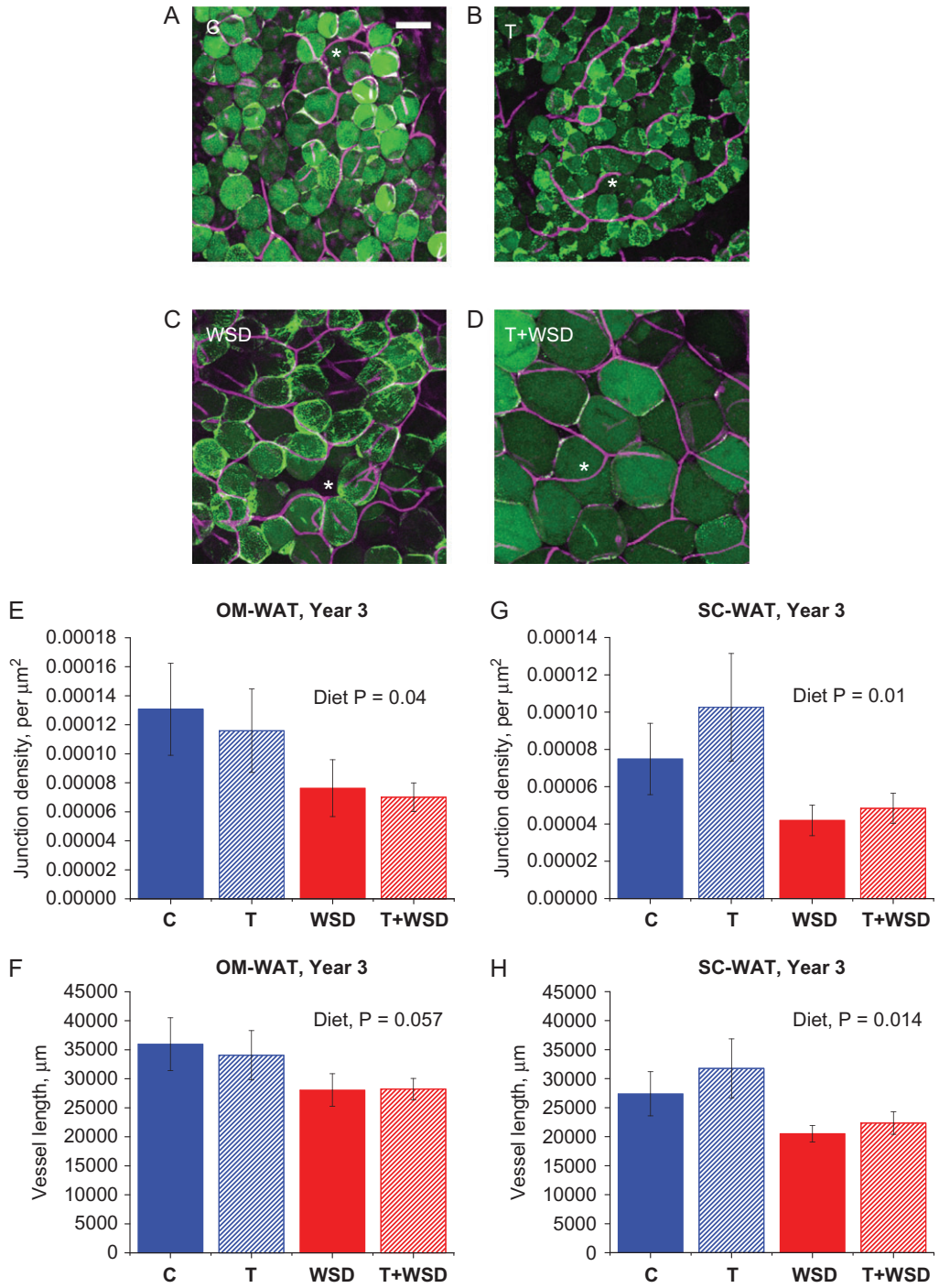

Figure 3 White adipose tissue (WAT) capillary networks. Omental (OM)-WAT biopsies collected in year 3 were co-labeled with BODIPY-C12 and Isolectin GS-IB4, Alexa Fluor™ 647 conjugate and analyzed by confocal microscopy as described in 'Materials and Methods.' (**A**–**D**) Representative images of OM-WAT; scale bar = 50 µm; asterisks, vessel junctions. Vessel junction density (**E** and **G**) and vessel length (**F** and **H**) were calculated for OM-WAT (E and F) and SC-WAT (G and H). Total vessel length in each WAT depot was calculated using ×10 images representing confocal slice with a 1550 × 1550 × 100-µm^3 dimension. Junction density is the number of junctions populating 1 µm^2 of a confocal projection. Overall effects of diet are indicated in inset above graphs.

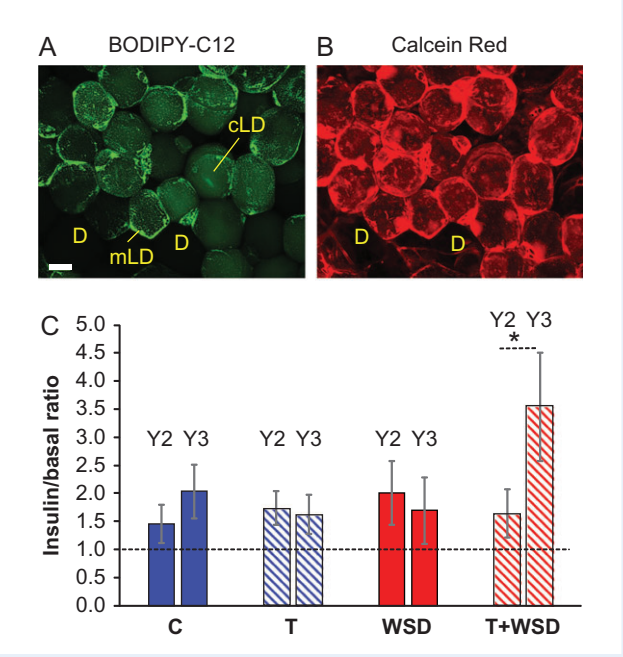

Figure 4 Free fatty acid uptake in omental white adipose tissue (OM-WAT). OM-WAT explants collected in years 2 and 3 were treated with basal or insulin-containing media, labeled with BODIPY-C12 (**A**) and live cell marker Calcein Red-Orange AM (**B**), fixed and processed for microscopy analysis as described in 'Materials and Methods.' (A and B) Representative confocal images of insulin-treated OM-WAT explants (scale bar = 50 μm). BODIPY-C12 is distributed to micro-lipid droplets (mLDs) and the central lipid droplet (cLD). Green fluorescence is excluded from red-negative dead adipocytes ('D'). (**C**) Quantification of insulin effects on BODIPY-C12 incorporation as a ratio of insulin-stimulated vs basal fluorescence. Bars are means ± SEM, $n = 6$–10 animals per group (average fluorescence per animal was calculated for 20–50 adipocytes). Asterisk, pair-wise comparison shows a statistically significant difference ($P < 0.05$) between years 2 and 3.

visceral adipocytes. Although previous studies demonstrated that women with PCOS have increased visceral adiposity (Manneras-Holm *et al.*, 2011; Gourgari *et al.*, 2015; Dumesic *et al.*, 2016), the effects of PCOS on the size of visceral adipocytes in humans is not yet reported. Consistent with our studies, rodent models of PCOS (McNeilly and Duncan, 2013) indicate that visceral adipocytes are also enlarged (Manneras *et al.*, 2008; Caldwell *et al.*, 2014; Kauffman *et al.*, 2015; Nohara *et al.*, 2013; Nikolic *et al.*, 2015). Studies in sheep (Padmanabhan and Veiga-Lopez, 2013) similarly reported enlarged adipocytes in intra-abdominal depots of prenatally androgenized female offspring (Veiga-Lopez *et al.*, 2013). Previous primate studies (Abbott *et al.*, 2013) did not observe significant effects of androgen excess on adipocyte size. However, this is potentially due the shorter duration of T + WSD treatment in one study (Varlamov *et al.*, 2013; McGee *et al.*, 2014) and a separate study employed a nonobesogenic, low-fat monkey chow diet in combination with prenatal T excess (Keller *et al.*, 2014).

We did not detect significant differences between treatment groups in the size of SC adipocytes. Although several studies indicate that PCOS is associated with enlarged SC adipocytes (Ek *et al.*, 1997; Faulds *et al.*, 2003; Manneras-Holm *et al.*, 2011), a recent human study showed no significant effect of PCOS on the average size of SC adipocytes (Dumesic *et al.*, 2016). However, the latter study reported the presence of a subpopulation of smaller SC adipocytes without a change in mean adipocyte size, which correlated with a degree of IR in lean PCOS patients (Dumesic *et al.*, 2016). Other studies also demonstrated that IR in normal obese (McLaughlin *et al.*, 2014) and PCOS obese (Keller *et al.*, 2014) patients is associated with accumulation of small SC adipocytes. Consequently, subtle changes in SC adipocyte fat storage due to androgen-mediated inhibition of preadipocyte differentiation with an increased proportion of small SC adipocytes (Chazenbalk *et al.*, 2012; Dumesic *et al.*, 2016; Keller *et al.*, 2014) could theoretically favor redistribution of free fatty acids to the visceral compartment, linking SC abdominal fat functional abnormalities with increased visceral adipocyte size.

WAT capillary system

WSD induced a significant reduction in capillary density in both WAT depots. The reduction in blood vessel length and junction densities in the WSD and T + WSD groups suggests that an obesogenic diet may impair WAT vascular development and capillary network expansion. Inadequate expansion of WAT capillary networks during diet-induced obesity is the principal factor responsible for the development of local hypoxia, inflammation and a major contributor to IR (Hosogai *et al.*, 2007; Pasarica *et al.*, 2009; Hodson *et al.*, 2013; Rausch *et al.*, 2008). The levels of the proinflammatory biomarker C-reactive protein (Pou *et al.*, 2007; Neeland *et al.*, 2013) were significantly elevated in both WSD groups (True *et al.*, 2017). This increase in C-reactive protein was correlated with reduced WAT capillary densities, which is thought to contribute to systemic inflammation and hypoxia (Pasarica *et al.*, 2009). Increased angiogenesis can protect against WAT hypoxia and metabolic complications in obese mice (Michailidou *et al.*, 2012; Robciuc *et al.*, 2016). There are no recent reports directly addressing vascular properties of WAT in PCOS patients and in related animal models; however, there are *in vitro* studies suggesting an increase in systemic angiogenesis in PCOS women (Tan *et al.*, 2010). Alterations in ovarian angiogenesis and vascularization are hypothesized to contribute to ovarian dysfunction in PCOS, including the manifestation of the PCO phenotype (Di Pietro *et al.*, 2015). Future studies employing functional *in vivo* and *in vitro*-based assays may distinguish whether endothelial and vascular properties of WAT are differentially affected by hyperandrogenemia and WSD, and if these effects are depot-specific.

Free fatty acid uptake in WAT

The present report suggests that hyperandrogenemia is associated with increased fatty acid uptake in OM-WAT, confirming a previous pilot study that female NHPs exposed to chronic hyperandrogenemia and acute WSD challenge display increased insulin-stimulated fatty acid uptake and increased insulin signaling in visceral WAT (Varlamov *et al.*, 2013). Our findings are also consistent with published data showing increased expression of the fatty acid transporter CD36 in OM-WAT of PCOS women (Seow *et al.*, 2009). Thus, increased fatty acid influx may contribute to the increased visceral obesity

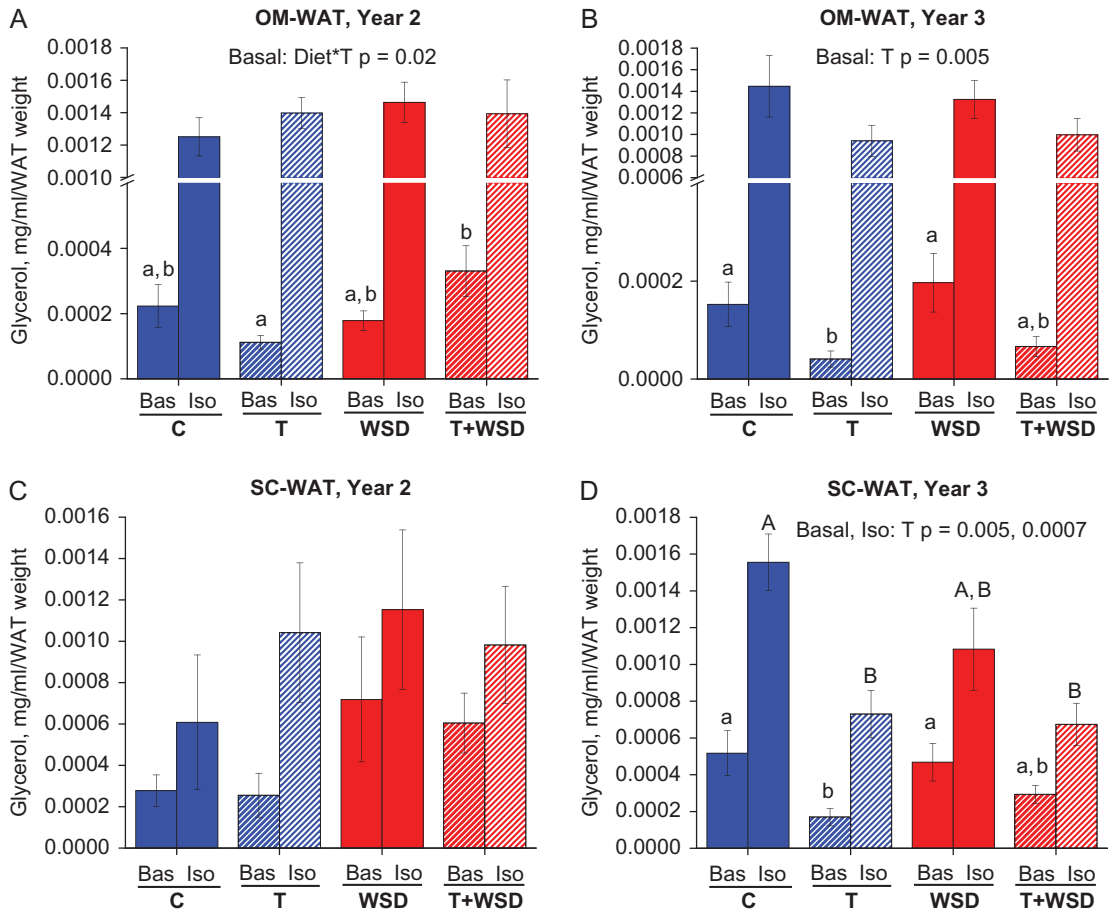

Figure 5 White adipose tissue (WAT) lipolysis. Omental (OM)-WAT (**A** and **B**) and sub-cutaneous (SC)-WAT (**C** and **D**) biopsies were collected in year 2 (A and C) and year 3 (B and D), divided into 50-mg explants, and treated for 2 h with basal (Bas) or isoproterenol (Iso)-containing media, in duplicate or triplicate. Conditioned media was used to determine glycerol release as described in 'Materials and Methods.' Lower-case letters indicate differences ($P < 0.05$) between treatments at Bas, and uppercase letters indicate differences between treatments cultured with Iso ($P < 0.05$). Bars are means ± SEM, $n = 6–10$ animals per group.

observed in PCOS women consuming obesogenic diets. It is also possible that increased fatty acid uptake is secondary to or concomitant with visceral adipocyte hypertrophy, which may develop as a result of suppressed lipolysis in the background of lipid-rich obesogenic diets.

WAT lipolysis

Hyperandrogenemia had an inhibitory effect on basal and isoproterenol-stimulated lipolysis in both fat depots under both dietary conditions. The suppression of fat cell lipolysis by androgen excess may represent the principal pathophysiological mechanism contributing to increased obesity in PCOS patients. Earlier studies employing SC-WAT biopsies obtained from women with PCOS and BMI-matched controls demonstrated that the former developed catecholamine-induced lipolytic resistance and had reduced β_2-adrenergic receptor levels (Ek *et al.*, 1997). Other studies also reported a reduction in β_2-adrenergic receptors expressed in SC adipocytes of PCOS patients and revealed additional defects such as a reduced capacity of endogenous protein kinase A to activate HSL (Faulds *et al.*, 2003), the principal lipase responsible for the β-adrenergic lipolytic response in WAT (Ryden *et al.*, 2007).

The data on visceral WAT lipolysis are more controversial. Ek *et al.* (2002) reported that OM-WAT obtained from PCOS patients had increased catecholamine-induced lipolysis, although our and other groups reported reduced HSL levels in visceral WAT in T-treated female NHPs (Varlamov *et al.*, 2013), as well as in WAT of PCOS patients (Seow *et al.*, 2009), respectively. Interestingly, OM-WAT from the T + WSD group obtained in year 2 displayed elevated basal lipolysis, while during the transition to year 3 this effect was reversed. These differences may be related to the duration of treatment or age-dependent remodeling of the local sympathetic innervation and ultimately the β-adrenergic lipolytic response in WAT might be different in younger versus older female primates (Zeng *et al.*, 2015; Zhu *et al.*, 2016).

One possible mechanism driving the development of catecholamine resistance in WAT is that elevated androgens induce the dysregulation of sympathetic tone in WAT in PCOS patients. Developmental

Table I Significant effects of hyperandrogenemia and Western-Style Diet (WSD) on white adipose tissue (WAT) morphology and function.

WAT-related process	T-specific	WSD-specific	T + WSD combined
Reduced basal lipolysis	+		
Reduced stimulated lipolysis	+		
Reduced blood vessel density		+	
Increased FFA uptake			+
Visceral adipocyte hypertrophy			+

Omental (OM)-WAT and sub-cutaneous (SC)-WAT display significantly reduced basal lipolysis after 3 years of exposure to hyperandrogenemia, and these effects were apparent on both chow and WSD. SC-WAT developed β-adrenergic lipolytic resistance following 3 years of treatment, which was also a diet-independent effect. In year 3, both WAT depots demonstrated reduced vessel length and junction densities in response to WSD, which was independent of hyperandrogenemia. The combination of hyperandrogenemia and WSD results in increased free fatty acid (FFA) uptake in OM-WAT (in year 3) and visceral OM-WAT hypertrophy (increase in adipocyte area). The combinatorial effect of hyperandrogenemia and WSD is associated with the greatest WAT dysfunction, including impaired lipolytic response, reduced capillary development and increased FFA uptake. These factors contribute to visceral obesity associated with the polycystic ovary syndrome (PCOS) phenotype.

androgen excess is associated with increased sympathetic tone in SC and visceral WAT in mice (Nohara *et al.*, 2013). Alterations in WAT sympathetic tone may represent a secondary effect of obesity and require further investigations, including defining the distribution of the local sympathetic innervation and the association with blood vessels, combined with functional assessment of sympathetic function in WAT.

Conclusions and future directions

In the United States, 80% of women with PCOS suffer from obesity and related metabolic complications (Legro *et al.*, 1999; Dumesic *et al.*, 2015), while the mechanisms contributing to excess body fat in these patients remain poorly understood. The present NHP study sheds light on the pathogenesis of obesity and adipose dysfunction observed in women with PCOS. The combined effects of hyperandrogenemia and consumption of WSD on WAT identified in the present study include impaired basal and β-adrenergic-stimulated lipolysis, increased insulin-stimulated fatty acid uptake and reduced blood vessel density (Table I), which collectively may contribute to the increased WAT hypertrophy and obesity observed in PCOS women.

Future studies will address the depot-specific biochemical, transcriptional and epigenetic effects of hyperandrogenemia and WSD. Specifically, we will elucidate the mechanisms underlying visceral fat hypertrophy and the potential development of adipocyte hyperplasia in response to hypoandrogenemia and WSD. We will also evaluate the effects of these treatments on the epigenetic profiles and differentiation and functional properties of adipose mesenchymal stem cells in this cohort of monkeys.

Acknowledgments

We thank the NCTRI Nonhuman Primate core, directed by Dr. Ov Slayden, the ONPRC Imaging and Morphology Support Core for technical assistance, Division of Comparative Medicine's Surgical Services Unit for performing all surgical procedures described in this manuscript and post-surgical monitoring of macaques, and Dr. Richard Stouffer and Dr. Daniel Dumesic for critical reading of the article.

Authors' roles

O.V. designed the study, conducted experiments and wrote the article, C.V.B. and S.S. analyzed the data, M.H., D.T. and A.W. conducted experiments, C.T.R. designed the study and wrote the article.

Funding

Research reported in this publication was supported by the Eunice Kennedy Shriver National Institute of Child Health and Human Development of the National Institutes of Health under award number P50 HD071836 to CTR and award number OD 011092 from the Office of the Director, National Institutes of Health, for operation of the Oregon National Primate Research Center. The content is solely the responsibility of the authors and does not necessarily represent the official views of the National Institutes of Health.

Conflict of interest

The authors have no conflicts of interest to declare.

References

Abbott DH, Nicol LE, Levine JE, Xu N, Goodarzi MO, Dumesic DA. Nonhuman primate models of polycystic ovary syndrome. *Mol Cell Endocrinol* 2013;**373**:21–28.

Azziz R, Carmina E, Dewailly D, Diamanti-Kandarakis E, Escobar-Morreale HF, Futterweit W, Janssen OE, Legro RS, Norman RJ, Taylor AE *et al.* The Androgen Excess and PCOS Society criteria for the polycystic ovary syndrome: the complete task force report. *Fertil Steril* 2009;**91**:456–488.

Barber TM, Franks S. Adipocyte biology in polycystic ovary syndrome. *Mol Cell Endocrinol* 2013;**373**:68–76.

Burt Solorzano CM, Beller JP, Abshire MY, Collins JS, McCartney CR, Marshall JC. Neuroendocrine dysfunction in polycystic ovary syndrome. *Steroids* 2012;**77**:332–337.

Caldwell AS, Middleton LJ, Jimenez M, Desai R, McMahon AC, Allan CM, Handelsman DJ, Walters KA. Characterization of reproductive, metabolic, and endocrine features of polycystic ovary syndrome in female hyperandrogenic mouse models. *Endocrinology* 2014;**155**:3146–3159.

Cameron JL, Jain R, Rais M, White AE, Beer TM, Kievit P, Winters-Stone K, Messaoudi I, Varlamov O. Perpetuating effects of androgen deficiency on insulin resistance. *Int J Obes (Lond)* 2016;**40**:1856–1863.

Chazenbalk G, Chen YH, Heneidi S, Lee JM, Pall M, Chen YD, Azziz R. Abnormal expression of genes involved in inflammation, lipid metabolism, and Wnt signaling in the adipose tissue of polycystic ovary syndrome. *J Clin Endocrinol Metab* 2012;**97**:E765–E770.

Chen YH, Heneidi S, Lee JM, Layman LC, Stepp DW, Gamboa GM, Chen BS, Chazenbalk G, Azziz R. miRNA-93 inhibits GLUT4 and is overexpressed in adipose tissue of polycystic ovary syndrome patients and women with insulin resistance. *Diabetes* 2013;**62**:2278–2286.

Chu M, Sampath H, Cahana DY, Kahl CA, Somwar R, Cornea A, Roberts CT Jr, arlamov O. Spatiotemporal dynamics of triglyceride storage in unilocular adipocytes. *Mol Biol Cell* 2014;**25**:4096–4105.

Ciaraldi TP, Aroda V, Mudaliar S, Chang RJ, Henry RR. Polycystic ovary syndrome is associated with tissue-specific differences in insulin resistance. *J Clin Endocrinol Metab* 2009;**94**:157–163.

Ciaraldi TP, el-Roeiy A, Madar Z, Reichart D, Olefsky JM, Yen SS. Cellular mechanisms of insulin resistance in polycystic ovarian syndrome. *J Clin Endocrinol Metab* 1992;**75**:577–583.

Di Pietro M, Parborell F, Irusta G, Pascuali N, Bas D, Bianchi MS, Tesone M, Abramovich D. Metformin regulates ovarian angiogenesis and follicular development in a female polycystic ovary syndrome rat model. *Endocrinology* 2015;**156**:1453–1463.

Diamanti-Kandarakis E, Dunaif A. Insulin resistance and the polycystic ovary syndrome revisited: an update on mechanisms and implications. *Endocr Rev* 2012;**33**:981–1030.

Diamanti-Kandarakis E, Panidis D. Unravelling the phenotypic map of polycystic ovary syndrome (PCOS): a prospective study of 634 women with PCOS. *Clin Endocrinol (Oxf)* 2007;**67**:735–742.

Diamond MP, Grainger D, Diamond MC, Sherwin RS, Defronzo RA. Effects of methyltestosterone on insulin secretion and sensitivity in women. *J Clin Endocrinol Metab* 1998;**83**:4420–4425.

Dumesic DA, Akopians AL, Madrigal VK, Ramirez E, Margolis DJ, Sarma MK, Thomas AM, Grogan TR, Haykal R, Schooler TA *et al*. Hyperandrogenism accompanies increased intra-abdominal fat storage in normal weight polycystic ovary syndrome women. *J Clin Endocrinol Metab* 2016;**101**:4178–4188.

Dumesic DA, Oberfield SE, Stener-Victorin E, Marshall JC, Laven JS, Legro RS. Scientific statement on the diagnostic criteria, epidemiology, pathophysiology, and molecular genetics of polycystic ovary syndrome. *Endocr Rev* 2015;**36**:487–525.

Dunaif A, Segal KR, Shelley DR, Green G, Dobrjansky A, Licholai T. Evidence for distinctive and intrinsic defects in insulin action in polycystic ovary syndrome. *Diabetes* 1992;**41**:1257–1266.

Eagleson CA, Bellows AB, Hu K, Gingrich MB, Marshall JC. Obese patients with polycystic ovary syndrome: evidence that metformin does not restore sensitivity of the gonadotropin-releasing hormone pulse generator to inhibition by ovarian steroids. *J Clin Endocrinol Metab* 2003;**88**:5158–5162.

Ek I, Arner P, Bergqvist A, Carlstrom K, Wahrenberg H. Impaired adipocyte lipolysis in nonobese women with the polycystic ovary syndrome: a possible link to insulin resistance? *J Clin Endocrinol Metab* 1997;**82**:1147–1153.

Ek I, Arner P, Ryden M, Holm C, Thorne A, Hoffstedt J, Wahrenberg H. A unique defect in the regulation of visceral fat cell lipolysis in the polycystic ovary syndrome as an early link to insulin resistance. *Diabetes* 2002;**51**:484–492.

Escobar-Morreale HF, San Millan JL. Abdominal adiposity and the polycystic ovary syndrome. *Trends Endocrinol Metab* 2007;**18**:266–272.

Faulds G, Ryden M, Ek I, Wahrenberg H, Arner P. Mechanisms behind lipolytic catecholamine resistance of subcutaneous fat cells in the polycystic ovarian syndrome. *J Clin Endocrinol Metab* 2003;**88**:2269–2273.

Gambineri A, Pelusi C, Genghini S, Morselli-Labate AM, Cacciari M, Pagotto U, Pasquali R. Effect of flutamide and metformin administered alone or in combination in dieting obese women with polycystic ovary syndrome. *Clin Endocrinol (Oxf)* 2004;**60**:241–249.

Gourgari E, Lodish M, Shamburek R, Keil M, Wesley R, Walter M, Sampson M, Bernstein S, Khurana D, Lyssikatos C *et al*. Lipoprotein particles in adolescents and young women with PCOS provide insights into their cardiovascular risk. *J Clin Endocrinol Metab* 2015;**100**:4291–4298.

Grayson BE, Levasseur PR, Williams SM, Smith MS, Marks DL, Grove KL. Changes in melanocortin expression and inflammatory pathways in fetal offspring of nonhuman primates fed a high-fat diet. *Endocrinology* 2010;**151**:1622–1632.

Hodson L, Humphreys SM, Karpe F, Frayn KN. Metabolic signatures of human adipose tissue hypoxia in obesity. *Diabetes* 2013;**62**:1417–1425.

Holte J, Bergh T, Berne C, Wide L, Lithell H. Restored insulin sensitivity but persistently increased early insulin secretion after weight loss in obese women with polycystic ovary syndrome. *J Clin Endocrinol Metab* 1995;**80**:2586–2593.

Hosogai N, Fukuhara A, Oshima K, Miyata Y, Tanaka S, Segawa K, Furukawa S, Tochino Y, Komuro R, Matsuda M *et al*. Adipose tissue hypoxia in obesity and its impact on adipocytokine dysregulation. *Diabetes* 2007;**56**:901–911.

Kauffman AS, Thackray VG, Ryan GE, Tolson KP, Glidewell-Kenney CA, Semaan SJ, Poling MC, Iwata N, Breen KM, Duleba AJ *et al*. A novel letrozole model recapitulates both the reproductive and metabolic phenotypes of polycystic ovary syndrome in female mice. *Biol Reprod* 2015;**93**:69.

Keller E, Chazenbalk GD, Aguilera P, Madrigal V, Grogan T, Elashoff D, Dumesic DA, Abbott DH. Impaired preadipocyte differentiation into adipocytes in subcutaneous abdominal adipose of PCOS-like female rhesus monkeys. *Endocrinology* 2014;**155**:2696–2703.

Legro RS, Kunselman AR, Dodson WC, Dunaif A. Prevalence and predictors of risk for type 2 diabetes mellitus and impaired glucose tolerance in polycystic ovary syndrome: a prospective, controlled study in 254 affected women. *J Clin Endocrinol Metab* 1999;**84**:165–169.

Lim SS, Norman RJ, Davies MJ, Moran LJ. The effect of obesity on polycystic ovary syndrome: a systematic review and meta-analysis. *Obes Rev* 2013;**14**:95–109.

Manneras-Holm L, Leonhardt H, Kullberg J, Jennische E, Oden A, Holm G, Hellstrom M, Lonn L, Olivecrona G, Stener-Victorin E *et al*. Adipose tissue has aberrant morphology and function in PCOS: enlarged adipocytes and low serum adiponectin, but not circulating sex steroids, are strongly associated with insulin resistance. *J Clin Endocrinol Metab* 2011;**96**:E304–E311.

Manneras L, Jonsdottir IH, Holmang A, Lonn M, Stener-Victorin E. Low-frequency electro-acupuncture and physical exercise improve metabolic disturbances and modulate gene expression in adipose tissue in rats with dihydrotestosterone-induced polycystic ovary syndrome. *Endocrinology* 2008;**149**:3559–3568.

Marsden PJ, Murdoch A, Taylor R. Severe impairment of insulin action in adipocytes from amenorrheic subjects with polycystic ovary syndrome. *Metabolism* 1994;**43**:1536–1542.

McGee WK, Bishop CV, Pohl CR, Chang RJ, Marshall JC, Pau FK, Stouffer RL, Cameron JL. Effects of hyperandrogenemia and increased adiposity on reproductive and metabolic parameters in young adult female monkeys. *Am J Physiol Endocrinol Metab* 2014;**306**:E1292–E1304.

McLaughlin T, Lamendola C, Coghlan N, Liu TC, Lerner K, Sherman A, Cushman SW. Subcutaneous adipose cell size and distribution: relationship to insulin resistance and body fat. *Obesity (Silver Spring)* 2014;**22**:673–680.

McNeilly AS, Duncan WC. Rodent models of polycystic ovary syndrome. *Mol Cell Endocrinol* 2013;**373**:2–7.

Mehrabani HH, Salehpour S, Amiri Z, Farahani SJ, Meyer BJ, Tahbaz F. Beneficial effects of a high-protein, low-glycemic-load hypocaloric diet in overweight and obese women with polycystic ovary syndrome: a randomized controlled intervention study. *J Am Coll Nutr* 2012;**31**:117–125.

Michailidou Z, Turban S, Miller E, Zou X, Schrader J, Ratcliffe PJ, Hadoke PW, Walker BR, Iredale JP, Morton NM *et al*. Increased angiogenesis protects against adipose hypoxia and fibrosis in metabolic disease-resistant 11beta-hydroxysteroid dehydrogenase type 1 (HSD1)-deficient mice. *J Biol Chem* 2012;**287**:4188–4197.

Michaud A, Boulet MM, Veilleux A, Noel S, Paris G, Tchernof A. Abdominal subcutaneous and omental adipocyte morphology and its relation to gene expression, lipolysis and adipocytokine levels in women. *Metabolism* 2014;**63**:372–381.

Moro C, Pasarica M, Elkind-Hirsch K, Redman LM. Aerobic exercise training improves atrial natriuretic peptide and catecholamine-mediated lipolysis in obese women with polycystic ovary syndrome. *J Clin Endocrinol Metab* 2009;**94**:2579–2586.

Muir LA, Neeley CK, Meyer KA, Baker NA, Brosius AM, Washabaugh AR, Varban OA, Finks JF, Zamarron BF, Flesher CG *et al*. Adipose tissue fibrosis, hypertrophy, and hyperplasia: correlations with diabetes in human obesity. *Obesity (Silver Spring)* 2016;**24**:597–605.

Neeland IJ, Ayers CR, Rohatgi AK, Turer AT, Berry JD, Das SR, Vega GL, Khera A, McGuire DK, Grundy SM *et al*. Associations of visceral and abdominal subcutaneous adipose tissue with markers of cardiac and metabolic risk in obese adults. *Obesity (Silver Spring)* 2013;**21**:E439–E447.

Nikolic M, Macut D, Djordjevic A, Velickovic N, Nestorovic N, Bursac B, Antic IB, Macut JB, Matic G, Vojnovic Milutinovic D. Possible involvement of glucocorticoids in 5alpha-dihydrotestosterone-induced PCOS-like metabolic disturbances in the rat visceral adipose tissue. *Mol Cell Endocrinol* 2015;**399**:22–31.

Nohara K, Waraich RS, Liu S, Ferron M, Waget A, Meyers MS, Karsenty G, Burcelin R, Mauvais-Jarvis F. Developmental androgen excess programs sympathetic tone and adipose tissue dysfunction and predisposes to a cardiometabolic syndrome in female mice. *Am J Physiol Endocrinol Metab* 2013;**304**:E1321–E1330.

Padmanabhan V, Veiga-Lopez A. Sheep models of polycystic ovary syndrome phenotype. *Mol Cell Endocrinol* 2013;**373**:8–20.

Pasarica M, Sereda OR, Redman LM, Albarado DC, Hymel DT, Roan LE, Rood JC, Burk DH, Smith SR. Reduced adipose tissue oxygenation in human obesity: evidence for rarefaction, macrophage chemotaxis, and inflammation without an angiogenic response. *Diabetes* 2009;**58**:718–725.

Pasquali R, Antenucci D, Casimirri F, Venturoli S, Paradisi R, Fabbri R, Balestra V, Melchionda N, Barbara L. Clinical and hormonal characteristics of obese amenorrheic hyperandrogenic women before and after weight loss. *J Clin Endocrinol Metab* 1989;**68**:173–179.

Polderman KH, Gooren LJ, Asscheman H, Bakker A, Heine RJ. Induction of insulin resistance by androgens and estrogens. *J Clin Endocrinol Metab* 1994;**79**:265–271.

Pou KM, Massaro JM, Hoffmann U, Vasan RS, Maurovich-Horvat P, Larson MG, Keaney JFJr., Meigs JB, Lipinska I, Kathiresan S *et al*. Visceral and subcutaneous adipose tissue volumes are cross-sectionally related to markers of inflammation and oxidative stress: the Framingham Heart Study. *Circulation* 2007;**116**:1234–1241.

Rausch ME, Weisberg S, Vardhana P, Tortoriello DV. Obesity in C57BL/6J mice is characterized by adipose tissue hypoxia and cytotoxic T-cell infiltration. *Int J Obes (Lond)* 2008;**32**:451–463.

Robciuc MR, Kivela R, Williams IM, de Boer JF, van Dijk TH, Elamaa H, Tigistu-Sahle F, Molotkov D, Leppanen VM, Kakela R *et al*. VEGFB/VEGFR1-induced expansion of adipose vasculature counteracts obesity and related metabolic complications. *Cell Metab* 2016;**23**:712–724.

Rosenfield RL, Ehrmann DA. The pathogenesis of polycystic ovary syndrome (PCOS): the hypothesis of PCOS as functional ovarian hyperandrogenism revisited. *Endocr Rev* 2016;**37**:467–520.

Ryden M, Jocken J, van Harmelen V, Dicker A, Hoffstedt J, Wiren M, Blomqvist L, Mairal A, Langin D, Blaak E *et al*. Comparative studies of the role of hormone-sensitive lipase and adipose triglyceride lipase in human fat cell lipolysis. *Am J Physiol Endocrinol Metab* 2007;**292**:E1847–E1855.

Seow KM, Tsai YL, Hwang JL, Hsu WY, Ho LT, Juan CC. Omental adipose tissue overexpression of fatty acid transporter CD36 and decreased expression of hormone-sensitive lipase in insulin-resistant women with polycystic ovary syndrome. *Hum Reprod* 2009;**24**:1982–1988.

Solomon CG. The epidemiology of polycystic ovary syndrome. Prevalence and associated disease risks. *Endocrinol Metab Clin North Am* 1999;**28**:247–263.

Spritzer PM, Lecke SB, Satler F, Morsch DM. Adipose tissue dysfunction, adipokines, and low-grade chronic inflammation in polycystic ovary syndrome. *Reproduction* 2015;**149**:R219–R227.

Tan BK, Adya R, Farhatullah S, Chen J, Lehnert H, Randeva HS. Metformin treatment may increase omentin-1 levels in women with polycystic ovary syndrome. *Diabetes* 2010;**59**:3023–3031.

Tchernof A, Belanger C, Morisset AS, Richard C, Mailloux J, Laberge P, Dupont P. Regional differences in adipose tissue metabolism in women: minor effect of obesity and body fat distribution. *Diabetes* 2006;**55**:1353–1360.

Thomson RL, Buckley JD, Noakes M, Clifton PM, Norman RJ, Brinkworth GD. The effect of a hypocaloric diet with and without exercise training on body composition, cardiometabolic risk profile, and reproductive function in overweight and obese women with polycystic ovary syndrome. *J Clin Endocrinol Metab* 2008;**93**:3373–3380.

True CA, Takahashi DL, Burns SE, Mishler EC, Bond KR, Wilcox MC, Calhoun AR, Bader LA, Dean TA *et al*. Chronic combined hyperandrogenemia and western-style diet in young female rhesus macaques causes greater metabolic impairments compared to either treatment alone. *Hum Reprod* 2017;**32**:1880–1891.

Varlamov O, Chu M, Cornea A, Sampath H, Roberts CTJr. Cell-autonomous heterogeneity of nutrient uptake in white adipose tissue of rhesus macaques. *Endocrinology* 2015;**156**:80–89.

Varlamov O, Chu MP, McGee WK, Cameron JL, O'Rourke RW, Meyer KA, Bishop CV, Stouffer RL, Roberts CTJr. Ovarian cycle-specific regulation of adipose tissue lipid storage by testosterone in female nonhuman primates. *Endocrinology* 2013;**154**:4126–4135.

Veiga-Lopez A, Moeller J, Patel D, Ye W, Pease A, Kinns J, Padmanabhan V. Developmental programming: impact of prenatal testosterone excess on insulin sensitivity, adiposity, and free fatty acid profile in postpubertal female sheep. *Endocrinology* 2013;**154**:1731–1742.

Wagenknecht LE, Langefeld CD, Scherzinger AL, Norris JM, Haffner SM, Saad MF, Bergman RN. Insulin sensitivity, insulin secretion, and abdominal fat: the Insulin Resistance Atherosclerosis Study (IRAS) Family Study. *Diabetes* 2003;**52**:2490–2496.

Wu HL, Heneidi S, Chuang TY, Diamond MP, Layman LC, Azziz R, Chen YH. The expression of the miR-25/93/106b family of micro-RNAs in the adipose tissue of women with polycystic ovary syndrome. *J Clin Endocrinol Metab* 2014;**99**:E2754–E2761.

Zeng W, Pirzgalska RM, Pereira MM, Kubasova N, Barateiro A, Seixas E, Lu YH, Kozlova A, Voss H, Martins GG *et al*. Sympathetic neuro-adipose connections mediate leptin-driven lipolysis. *Cell* 2015;**163**:84–94.

Zhu Y, Gao Y, Tao C, Shao M, Zhao S, Huang W, Yao T, Johnson JA, Liu T, Cypess AM *et al*. Connexin 43 mediates white adipose tissue beiging by facilitating the propagation of sympathetic neuronal signals. *Cell Metab* 2016;**24**:420–433.

Zudaire E, Gambardella L, Kurcz C, Vermeren S. A computational tool for quantitative analysis of vascular networks. *PLoS One* 2011;**6**:e27385.